PHYSIOME
journal.physiomeproject.org
ISSN: 2744-6204

Reproducibility of a Digital Twin of the Angiotensin II Receptor Blocker Losartan

Mariia Myshkina[1], Michelle Elias[1], Ennie Tensil[2], and Matthias König[1,3*]

[1]Humboldt-Universität zu Berlin, Faculty of Life Sciences, Department of Biology, Systems Medicine of the Liver, Unter den Linden 6, 10099 Berlin, Germany
[2]Charité – Universitätsmedizin Berlin, corporate member of Freie Universität Berlin and Humboldt-Universität zu Berlin, Charitéplatz 1, 10117 Berlin, Germany
[3]University of Stuttgart, Institute of Structural Mechanics and Dynamics in Aerospace Engineering, Pfaffenwaldring 27, 70569 Stuttgart, Germany

ORIGINAL

Abstract
A digital twin in the form of a whole-body physiologically based pharmacokinetic/pharmacodynamic (PBPK/PD) model of losartan was developed to systematically evaluate the influence of patient-specific factors on drug disposition and effects. Based on curated data from 25 clinical studies, the model simulates the absorption, distribution, metabolism and excretion (ADME) as well as pharmacological effects of the drug. The model accounts for variability caused by the differences in renal and hepatic function, and by genetic polymorphisms of CYP2C9 and ABCB1. The model is implemented in the Systems Biology Markup Language (SBML) standard. Simulations were performed utilising the libroadrunner library. Here, we demonstrate the computational reproducibility of the key findings from the primary publication, thereby verifying the consistency and reproducibility of the model implementation with the published results.

Keywords: Losartan, PBPK/PD, SBML, Pharmacokinetics, Pharmacodynamics, Computational Model

Curated Model Implementation
https://doi.org/10.5281/zenodo.18213663

Primary Publications
E. Tensil, M. Myshkina, and M. König. A Digital Twin of the Angiotensin II Receptor Blocker Losartan: Physiologically Based Modeling of Blood Pressure Regulation. *Pharmaceutics*, Jan. 2026.

1 Introduction

In the primary publication (Tensil et al., 2026), we developed a whole-body physiologically based pharmacokinetic/pharmacodynamic (PBPK/PD) model of losartan, an inhibitor of angiotensin II receptor used for the treatment of arterial hypertension (Lo et al., 1995; Sica et al., 2005). The goal of the study was to mechanistically integrate the key factors driving variability of its pharmacokinetics and pharmacodynamics. The model accounts for effects of renal (Pedro et al., 2000; Sica et al., 1995; Yoshitani et al., 2002) and hepatic (McIntyre et al., 1997; Sica et al., 2005) function, and of CYP2C9 and ABCB1 genetic polymorphisms (Fischer et al., 2002; Göktaş et al., 2016; Haufroid, 2011; Lo et al., 1995; Sekino et al., 2003; Shin et al., 2020; Yasar et al., 2002b). The model's structure and parameters were derived from a comprehensive dataset consisting of 25 published clinical studies. The data from these studies were digitised, analysed, and uploaded to the pharmacokinetics database PK-DB (Grzegorzewski et al., 2021). The model's development and scientific validation are described in detail in the primary paper (Tensil et al., 2026).

OPEN ACCESS
Reproducible Model

Corresponding author
koenigmx@hu-berlin.de

Here, we present the original model and the accompanying scripts. The model is encoded in the Systems Biology Markup Language (SBML) (Hucka et al., 2019; Keating et al., 2020). The scripts allow running the simulations and reproducing the key results presented in the primary publication.

2 Model Description

A schematic overview of the model structure is provided in Figure 1.

The disposition of losartan is described using a whole-body physiologically based pharmacokinetic/pharmacodynamic (PBPK/PD) model. The model integrates four submodels. Three of them represent the main organs involved in the pharmacokinetics and metabolism of losartan (intestine, liver, and kidneys), with the fourth one describing the pharmacodynamics. The gastrointestinal tract model simulates the dissolution of orally administered losartan, its subsequent first-order absorption, and fecal excretion of the drug and its main metabolites. In the liver submodel, losartan is converted by the CYP2C9/3A4 enzymes to its active metabolite E3174. The following conversion of the E3174 to an inactive metabolite, L158, is catalysed by the UDP-glucuronosyltransferase. All three substances, losartan, E3174, and L158, are exported to the systemic circulation, which interconnects all three submodels. Moreover, losartan and its metabolites are excreted in bile into the intestinal lumen. The kidney model implements the renal excretion of these substances.

The pharmacodynamic submodel of losartan represents the main components of the renin-angiotensin-aldosterone system (RAAS). The pharmacodynamic effect of E3174 is modelled through an inhibition of the effect of angiotensin II on aldosterone secretion and an activation of renin secretion.

The model accounts for patient-specific factors through scaling of corresponding parameters. Renal impairment was modelled as a progressive decline in renal function by scaling the factor f_{renal}. Hepatic impairment was implemented as progressive cirrhosis by scaling liver function with the parameter $f_{cirrhosis}$. CYP2C9 and ABCB1 genetic variability was incorporated using allele-specific activity scaling with the corresponding parameters f_{cyp2c9} and f_{abcb1}. All parameters were adjusted according to the published data.

The PBPK/PD model and its submodels were developed using the Systems Biology Markup Language (SBML) (Hucka et al., 2019; Keating et al., 2020). Programming and visualisation of the models were performed using the `sbmlutils` (König, 2024) and `cy3sbml` (König et al., 2012) libraries. Numerical solutions for the ordinary differential equations (ODEs) underlying the model were computed using `sbmlsim` (König, 2021), which is powered by the high-performance SBML simulation engine `libroadrunner` (Welsh et al., 2023; Somogyi et al., 2015). The submodels were developed as SBML submodels and coupled with the whole-body model using the hierarchical model composition (comp) SBML extension (Smith et al., 2015). The complete model and submodels reference simulations and visualisations are available as a COMBINE archive (OMEX) (Bergmann et al., 2014, 2015). The model is annotated with extensive metadata using the open modeling and exchange (OMEX) metadata specification (Neal et al., 2020, 2019). The model was validated using the SBML validator, with the model passing all validation tests without errors or warnings. The FAIRness of the model was increased by following the FAIRification of computational models in the biological workflow (Balaur et al., 2025).

The model and all associated materials (mathematical formulation, simulation scripts, parameters, and documentation) are publicly available in SBML format and OMEX archive under a CC-BY 4.0 license at https://github.com/matthiaskoenig/losartan-model, with version 0.8.0 used in the publication and for model validation.

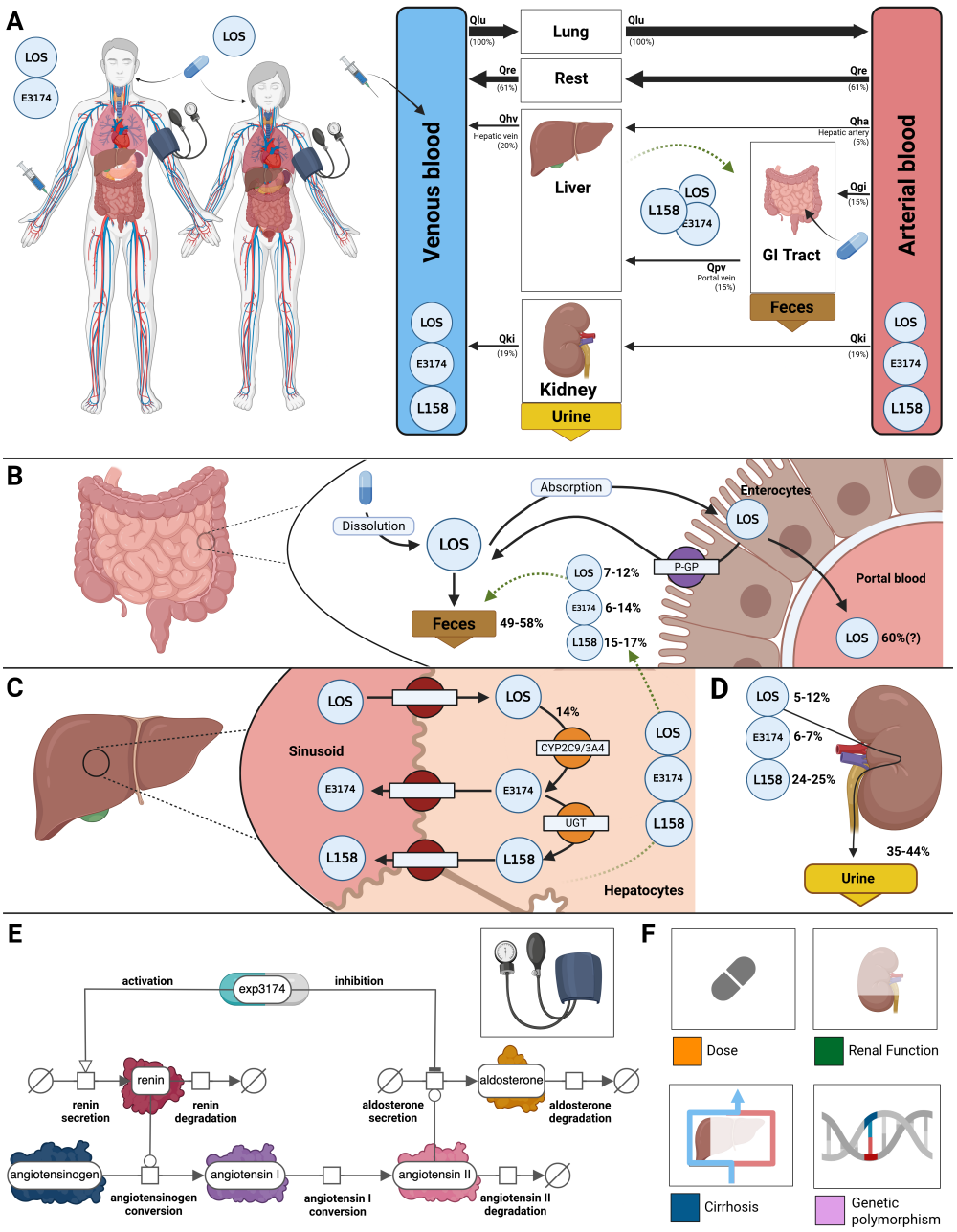

Figure 1. Whole-body PBPK/PD model of losartan.

A) Whole body model showing circulation via the arterial and venous blood, with organs (liver, gastrointestinal (GI) tract, kidneys) influencing the pharmacokinetics of losartan (LOS). **B)** Intestine model describing the dissolution and absorption of LOS by enterocytes and the P-glycoprotein-mediated efflux back into the intestine. Approximately 50-60% of the dose is excreted as losartan or its metabolites (E3174 and L158). **C)** Hepatic model depicting the uptake of losartan by hepatocytes and its conversion by cytochrome p450 2C9 and 3A4 (CYP2C9, CYP3A4) to losartan carboxylic acid (E3174, 14% of the losartan dose) and the following conversion by UDP-glucuronosyltransferase (UGT) to L158. Losartan and its metabolites can re-enter the intestinal model via biliary export. **D)** Renal model showing excretion of losartan, E3174 and L158 via urine, approximately 5-12%, 6-7% and 24-25% of the losartan dose, respectively. **E)** Pharmacodynamic model of E3174 acting on the RAAS. **F)** Key factors influencing losartan PK and PD profiles are accounted for in the model. Illustrations for losartan dose dependency, renal and hepatic impairments, and genetic polymorphisms.

3 Computational Simulation

All simulations were performed using Python 3.14 together with the high-performance `libroadrunner` simulation engine. The workflow was tested across multiple platforms, including Ubuntu 24.04/25.10 and Windows 11. For SBML model handling and simulation, we relied on the `sbmlutils` and `sbmlsim` libraries, while data management and figure generation were carried out with standard scientific Python packages.

To ensure reproducibility, we provide two equivalent setups for regenerating all figures presented in Section 4: (1) a local Python installation using uv, and (2) a containerised workflow using Docker. Both approaches reproduce all results from the primary publication. Reproducibility is continuously validated through automated integration tests, with results available at https://github.com/matthiaskoenig/losartan-model/actions.

3.1 Python with uv (local install)

This workflow installs the package directly on your machine using uv.

Prerequisite: uv must be installed on your system (https://docs.astral.sh/uv/getting-started/installation/).

Clone the repository, move into its folder, and checkout correct version:

```
git clone https://github.com/matthiaskoenig/losartan-model.git
cd losartan-model
git checkout 0.8.0
```

Set up the uv virtual environment and install all dependencies:

```
uv sync
```

Run the full analysis:

```
uv run run_losartan -a all -r results
```

All reproduced figures and outputs are written to `./results/` inside the repository.

Alternatively, you can use any other way to set up a local Python environment (e.g. conda) and install the package after cloning the repository via:

```
pip install -e .
```

or directly from the tag via:

```
pip install git+https://github.com/matthiaskoenig/losartan-model.git@0.8.0
```

The full analysis can be run in the Python environment via:

```
(env) run_losartan -a all -r results
```

3.2 Docker (containerised)

This workflow runs the analysis in a preconfigured Docker container.

Prerequisite: Docker must be installed on your system (https://docs.docker.com/get-docker/).

Start the container and mount a local `results/` directory:

```
docker run -v "${PWD}/results:/results" -it matthiaskoenig/losartan:0.8.0 /
    bin/bash
```

Inside the container, run the analysis. Results will be written to the mounted folder:

```
uv run run_losartan -a all -r /results
```

The reproduced figures and outputs are then accessible on the host system in `./results/`.

If file access is restricted on Linux due to permissions, adjust ownership and rights as follows:

```
sudo chown $(id -u):$(id -g) -R "${PWD}/results"
sudo chmod 775 "${PWD}/results"
```

3.3 Available Options

Specific parts of the analysis can be executed by providing command-line arguments. A full overview of the available options is obtained via:

```
uv run run_losartan --help
```

3.4 Outputs

The workflow reproduces all figures and results from the primary publication, including:

- Study simulations (Figures 2–3)
- Simulation experiments and scans (Figures 4–5)

All results are stored in the `results/` directory. This directory contains the individual figure panels in PNG format as well as an automatically generated HTML report (`index.html`) that consolidates all figures into a single document. The content of this report directly corresponds to Figures 2–5 in the manuscript.

4 Reproducibility Goals

The reproducibility of the losartan PBPK/PD model was confirmed by reproducing key figures from the original publication. The figures presented here are a selection chosen to demonstrate consistent reproduction of results across different dose levels and pathophysiological states, as well as across CYP2C9 and ABCB1 alleles. Tables 1–2 provide an overview of the simulation observables and the parameter changes specific to each study, experiment, or scan. The model and simulation scripts can be used to reproduce the full set of results from the original study.

Table 1. Plotted observables and parameter changes per study simulation. Square brackets around SBML species ids indicate concentrations (amount/volume units). Square brackets enclosing numerical values indicate parameter ranges, whereas curly brackets indicate sets of discrete choices.

StudyID	Plotted	Changes
Azizi1999 (Azizi et al., 1999)	[Cve_los], [Cve_e3174], [ren], [ang1], [ang2], MAP	PODOSE_los $\in \{0, 50\}$ mg ren_ref, [ren] = 58.5 pg/ml ang1_ref, [ang1] = 11.8 pg/ml ang2_ref, [ang2] = 7.2 pg/ml SBP_ref = 120 mmHg DBP_ref = 70.5 mmHg
Bae2011 (Bae et al., 2011)	[Cve_los], [Cve_e3174]	PODOSE_los = 50 mg LI__f_cyp2c9 $\in \{1.0, 0.17\}$
Doig1993 (Doig et al., 1993)	[ren], [ald], ald_change, ald_ratio, SPB, DBP	PODOSE_los $\in \{0, 5, 10, 25, 50, 100\}$ mg BW = 76.5 kg ren_ref, [ren] = 44.8 pg/ml ald_ref, [ald] = 774.12 pg/ml SBP_ref = 115 mmHg DBP_ref = 63.5 mmHg

Table 1. Plotted observables and parameter changes per study simulation (continued). Square brackets around SBML species ids indicate concentrations (amount/volume units). Square brackets enclosing numerical values indicate parameter ranges, whereas curly brackets indicate sets of discrete choices.

StudyID	Plotted (sid)	Changes
Donzelli2014 (Donzelli et al., 2014)	[Cve_los], [Cve_e3174]	PODOSE_los = 12.5 mg
FDA1995S60 (FDA, 1995a)	[Cve_los], Aurine_los, Afeces_los, [Cve_e3174], Aurine_e3174, Afeces_e3174, [Cve_l158], Aurine_l158, Afeces_l158, [Cve_total], Aurine_total, Afeces_total	PODOSE_los = 100 mg IVDOSE_los = 30 mg IVDOSE_e3174 = 20 mg BW = 78.6 kg
FDA1995S67 (FDA, 1995b)	[Cve_los], Aurine_los, [Cve_e3174], Aurine_e3174	PODOSE_los = 50 mg IVDOSE_los = 10 mg IVDOSE_e3174 = 10 mg BW = 82.3 kg f_cirrhosis $\in \{0.0, 0.67\}$
Fischer2002 (Fischer et al., 2002)	[Cve_los], Aurine_los, [Cve_e3174], Aurine_e3174	PODOSE_los = 50 mg BW = 72 kg
Goldberg1995 (Goldberg et al., 1995b)	[Cve_los], [Cve_e3174], [ren]	PODOSE_los $\in \{0, 50\}$ mg ren_ref, [ren] = 10.5 pg/ml
Goldberg1995a (Goldberg et al., 1995a)	[Cve_los], [Cve_e3174], [ren], [ang2], [ald], DBP_change	PODOSE_los $\in \{0, 25, 100\}$ mg ren_ref, [ren] = 5.02 pg/ml ang2_ref, [ang2] = 2.71 pg/ml ald_ref, [ald] = 11.2 ng/dl
Han2009a (Han et al., 2009)	[Cve_los], [Cve_e3174]	PODOSE_los = 50 mg LI__f_cyp2c9 $\in \{1.0, 0.585\}$
Huang2021 (Huang et al., 2021)	[Cve_los], [Cve_e3174]	PODOSE_los = 50 mg BW $\in \{54, 52\}$ kg LI__f_cyp2c9 $\in \{1.0, 0.585\}$
Kim2016 (Kim et al., 2016)	[Cve_los], [Cve_e3174]	PODOSE_los = 25 mg BW = 62.3 kg
Kobayashi2008 (Kobayashi et al., 2008)	[Cve_los], [Cve_e3174]	PODOSE_los = 50 mg
Lee2003b (Lee et al., 2003)	[Cve_los], [Cve_e3174]	PODOSE_los = 50 mg LI__f_cyp2c9 $\in \{1.0, 0.8, 0.585\}$
Li2009 (Li et al., 2009)	[Cve_los], [Cve_e3174]	PODOSE_los = 50 mg LI__f_cyp2c9 $\in \{1.0, 0.17, 0.525\}$

Table 1. Plotted observables and parameter changes per study simulation (continued). Square brackets around SBML species ids indicate concentrations (amount/volume units). Square brackets enclosing numerical values indicate parameter ranges, whereas curly brackets indicate sets of discrete choices.

StudyID	Plotted (sid)	Changes
Lo1995 (Lo et al., 1995)	[Cve_los], Aurine_los, [Cve_e3174], Aurine_e3174	PODOSE_los ∈ {50, 100} mg Ri_los ∈ {0.0, 1.0, 1.5} mg/min Ri_e3174 ∈ {0, 1} mg/min BW ∈ {75.6, 78.6} kg
Munafo1992 (Munafo et al., 1992)	[Cve_los], [Cve_e3174], [ald]	PODOSE_los ∈ {0, 40, 80, 120} mg BW = 66.5 kg
Oh2012 (Oh et al., 2012)	[Cve_los], [Cve_e3174], mr_e3174_los_plasma	PODOSE_los = 2 mg
Ohtawa1993 (Ohtawa et al., 1993)	[Cve_los], Aurine_los, [Cve_e3174], Aurine_e3174, [ren], [ang2], [ald], SBP, DBP	PODOSE_los ∈ {0, 25, 50, 100, 200} mg BW = 64.3 kg ren_ref, [ren] = 10 pg/ml ang2_ref, [ang2] = 10.3 pg/ml ald_ref, [ald] = 110.4 pg/ml SBP_ref = 116 mmHg DBP_ref = 70.5 mmHg
Puris2019 (Puris et al., 2019)	[Cve_los], [Cve_e3174]	PODOSE_los = 12.5 mg
Sekino2003 (Sekino et al., 2003)	mr_e3174_los_plasma, mr_e3174_los_urine, SBP_change, DBP_change	PODOSE_los = 25 mg BW ∈ {65.7, 61.7} kg LI__f_cyp2c9 ∈ {1.0, 0.585}
Shin2020 (Shin et al., 2020)	[Cve_los], [Cve_e3174], [Cve_los_e3174], Aurine_los_e3174	PODOSE_los = 50 mg BW = 67.4 kg GU__f_abcb1 ∈ {1.0, 0.306, 0.653}
Sica1995 (Sica et al., 1995)	[Cve_los], Aurine_los, [Cve_e3174], Aurine_e3174	PODOSE_los = 100 mg BW ∈ {84.6, 75.7, 75.4} kg KI__f_renal_function ∈ {0.14, 0.5, 0.95}
Tanaka2014 (Tanaka et al., 2014)	[Cve_los], [Cve_e3174], mr_e3174_los_plasma	PODOSE_los = 50 mg
Yasar2002a (Yasar et al., 2002a)	[Cve_los], Aurine_los, [Cve_e3174], Aurine_e3174, mr_e3174_los_urine	PODOSE_los ∈ {25, 50} mg LI__f_cyp2c9 ∈ {1.0, 0.17, 0.385, 0.585, 0.6, 0.8}

Table 2. Plotted observables and parameter changes per simulation experiment and scan. Square brackets around SBML species ids indicate concentrations (amount/volume units). Square brackets enclosing numerical values indicate parameter ranges, whereas curly brackets indicate sets of discrete choices.

Simulation	Plotted	Changes
DoseDependencyExperiment	[Cve_los], Aurine_los, Afeces_los, [Cve_e3174], Aurine_e3174, [Cve_l158], [ren], [ang1], [ald], SBP, DBP	PODOSE_los ∈ [10, 100] mg

Table 2. Plotted observables and parameter changes per simulation experiment (continued). Square brackets around SBML species ids indicate concentrations (amount/volume units). Square brackets enclosing numerical values indicate parameter ranges, whereas curly brackets indicate sets of discrete choices.

Simulation	Plotted (sid)	Changes
HepaticRenalImpairment	[Cve_los], Aurine_los, Afeces_los, [Cve_e3174], Aurine_e3174, [Cve_l158], [ren], [ang1], [ald], SBP, DBP	PODOSE_los = 50 mg KI__f_renal_function $\in [-1.0, 1.0]$ f_cirrhosis $\in [0.0, 0.9]$
GeneticPolymorphism	[Cve_los], Aurine_los, Afeces_los, [Cve_e3174], Aurine_e3174, [Cve_l158], [ren], [ang1], [ald], SBP, DBP	PODOSE_los = 50 mg LI__f_cyp2c9 $\in [-1.0, 1.0]$ GU__f_abcb1 $\in [-1.0, 1.0]$
LosartanParameterScan	PODOSE_los, f_cirrhosis, LI__f_cyp2c9, GU__f_abcb1, KI__f_renal_function, AUC_{inf}, C_{max}, half-life, SBP_{min}, DBP_{min}	PODOSE_los $\in [10, 100]$ mg KI__f_renal_function $\in [-1.0, 1.0]$ (PODOSE_los = 50 mg) f_cirrhosis $\in [0.0, 0.9]$ (PODOSE_los = 50 mg) LI__f_cyp2c9 $\in [-1.0, 1.0]$ (PODOSE_los = 50 mg) GU__f_abcb1 $\in [-1.0, 1.0]$ (PODOSE_los = 50 mg)

4.1 Reproduction of Study Simulations

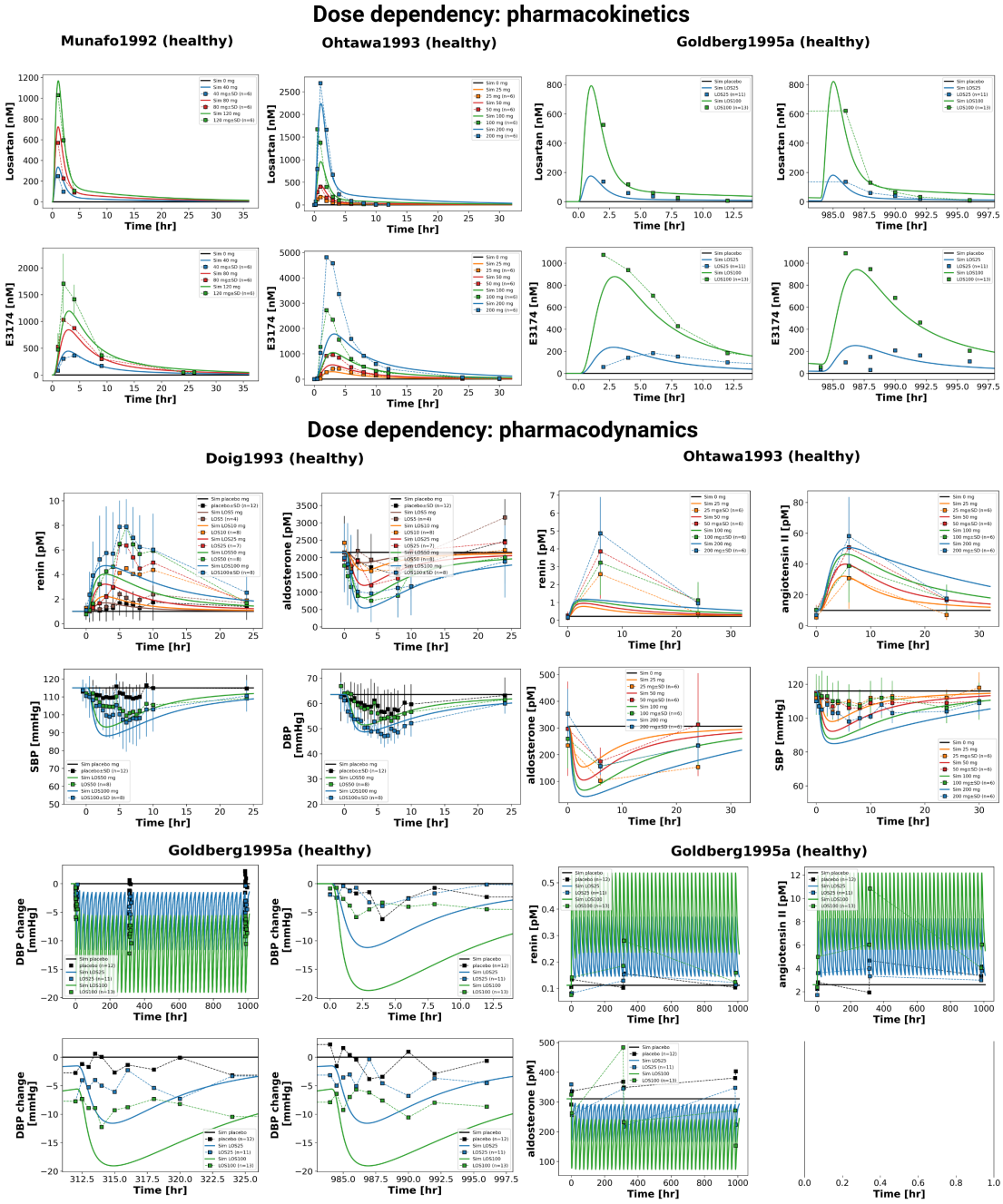

Figure 2. Reproduction of study simulations (dose dependency) from the primary publication. Data is taken from (Doig et al., 1993; Goldberg et al., 1995a; Munafo et al., 1992; Ohtawa et al., 1993).

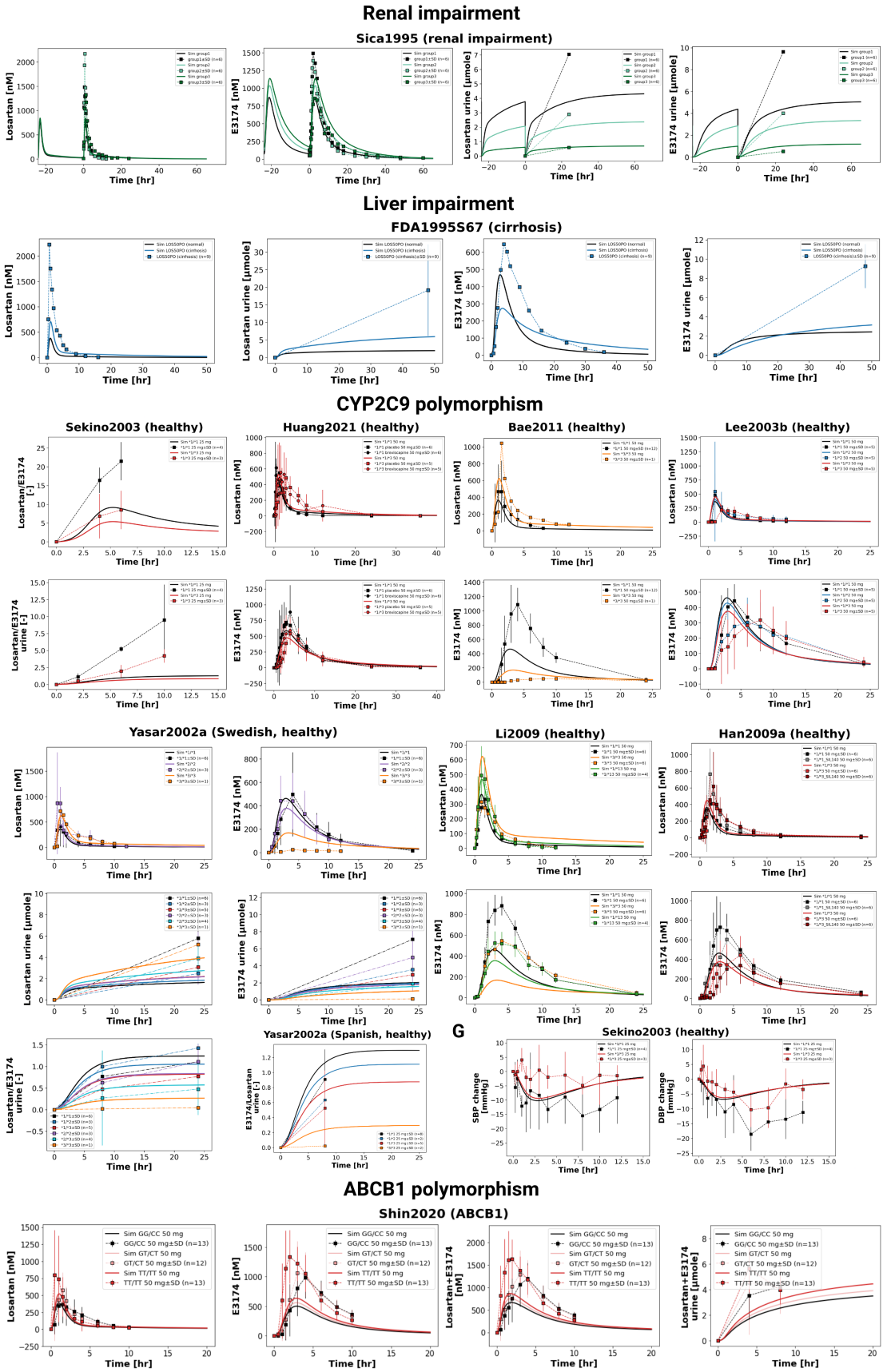

Figure 3. Reproduction of study simulations (renal and liver impairment, CYP2C9 and ABCB1 polymorphism) from the primary publication. Data is taken from (Bae et al., 2011; FDA, 1995b; Han et al., 2009; Huang et al., 2021; Lee et al., 2003; Li et al., 2009; Sekino et al., 2003; Shin et al., 2020; Sica et al., 1995; Yasar et al., 2002a).

4.2 Reproduction of Simulations, Experiments, and Scans

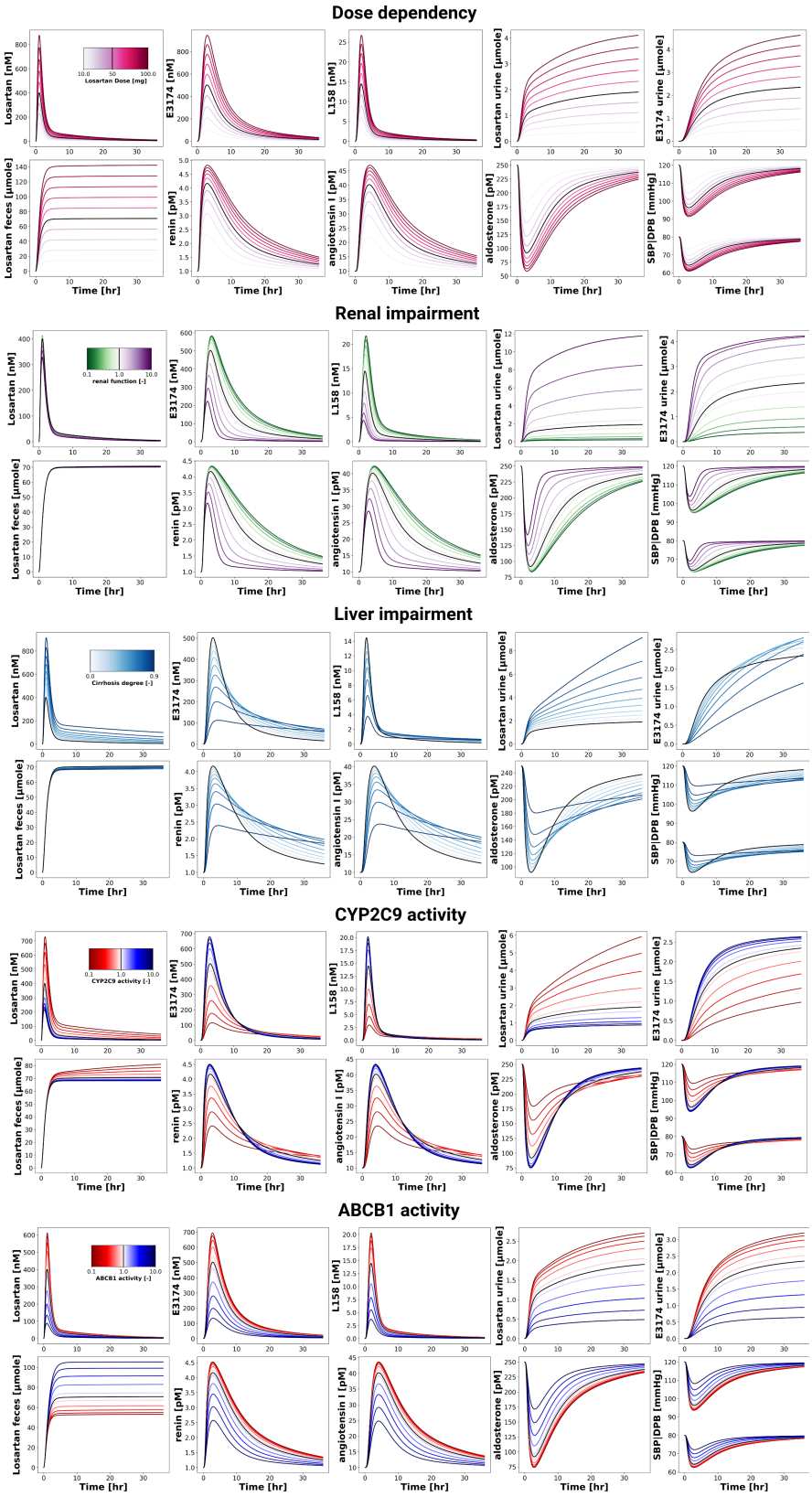

Figure 4. Reproduction of simulation experiments (dose dependency, renal and liver impairment, CYP2C9 and ABCB1 activity) from the primary publication.

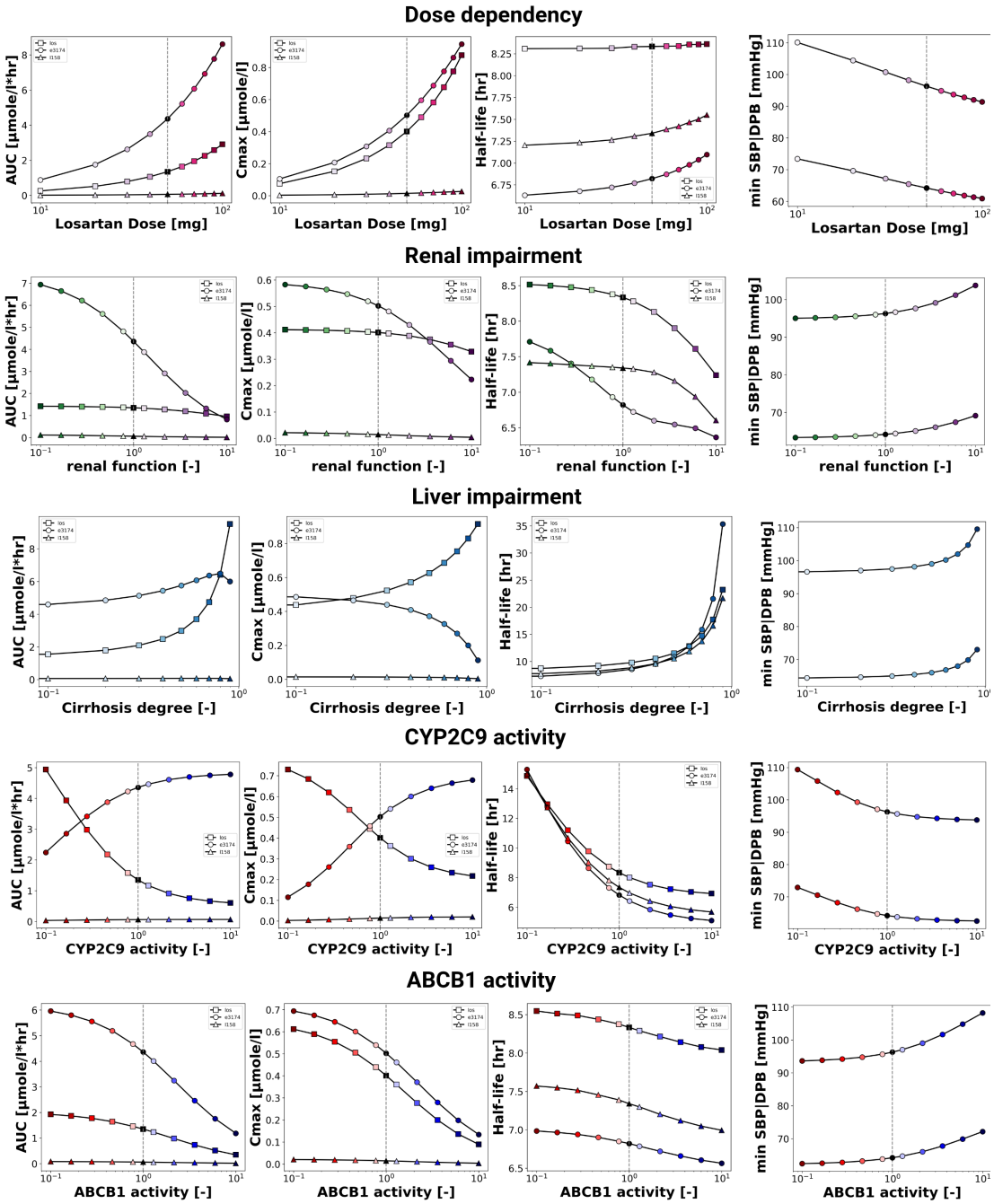

Figure 5. Reproduction of parameter scans (dose dependency, renal and liver impairment, CYP2C9 and ABCB1 activity) from the primary publication.

5 Discussion

We have demonstrated the computational reproducibility of the key findings from the losartan PBPK/PD model presented in the primary publication. Using the provided simulation scripts, all figures were regenerated without modifying parameters or structure, verifying the consistency of the model. Reproducibility was confirmed across different operating systems using both a local installation with uv and a Dockerized workflow. The uv-based approach allows users to install the package and dependencies natively. In addition, the containerised workflow provides a fully preconfigured environment and ensures consistent results independent of the local setup. Encoding the model in SBML with hierarchical composition removes ambiguity and allows modular

reuse of the submodels. Together with the use of community standards and FAIR practices, this provides a transparent and reusable resource that can be applied or extended in future pharmacokinetic/pharmacodynamic modeling work.

Author Contributions

E.T. and M.K. contributed to conceptualisation, methodology, data curation, and development of the PBPK/PD model. E.T., M.M., M.E., and M.K. contributed to analyses, software, and visualisation. M.M., M.E., and M.K. contributed to the reproducibility of the computational workflow. M.M. wrote the original draft. E.T., M.M., M.E., and M.K. contributed to the manuscript review and editing. M.K. provided supervision throughout the project. All authors approved the final manuscript.

Funding

Matthias König (MK) was supported by the Federal Ministry of Research, Technology and Space (BMFTR, Germany) within ATLAS by grant number 031L0304B and by the German Research Foundation (DFG) within the Research Unit Program FOR 5151 "QuaLiPerF (Quantifying Liver Perfusion-Function Relationship in Complex Resection - A Systems Medicine Approach)" by grant number 436883643 and by grant number 465194077 (Priority Programme SPP 2311, Subproject SimLivA). This work was supported by the BMBF-funded de.NBI Cloud within the German Network for Bioinformatics Infrastructure (de.NBI) (031A537B, 031A533A, 031A538A, 031A533B, 031A535A, 031A537C, 031A534A, 031A532B). Mariia Myshkina was supported by the Federal Ministry of Research, Technology and Space (BMFTR, Germany) within ATLAS by grant number 031L0304B and by the German Research Foundation (DFG) within the Priority Programme SPP 2311, Subproject SimLivA by grant number 465194077. Michelle Elias was supported by the German Research Foundation (DFG) within the Priority Programme SPP 2311, Subproject SimLivA by grant number 465194077.

Acknowledgments

Figures were created in BioRender. König, M. (2026) https://BioRender.com/qrimu54.

References

M. Azizi, G. Chatellier, T. T. Guyene, and J. Ménard. Pharmacokinetic-pharmacodynamic interactions of candesartan cilexetil and losartan. *Journal of hypertension*, 17(4):561–568, Apr. 1999. ISSN 0263-6352. doi: 10.1097/00004872-199917040-00015.

J.-w. Bae, C.-i. Choi, M.-j. Kim, D.-h. Oh, S.-k. Keum, J.-i. Park, B.-h. Kim, H.-k. Bang, S.-g. Oh, B.-s. Kang, H.-j. Park, H.-d. Kim, J.-h. Ha, H.-j. Shin, Y.-h. Kim, H.-s. Na, M.-w. Chung, C.-g. Jang, and S.-y. Lee. Frequency of CYP2C9 alleles in Koreans and their effects on losartan pharmacokinetics. *Acta pharmacologica Sinica*, 32(10):1303–1308, Oct. 2011. ISSN 1745-7254 1671-4083. doi: 10.1038/aps.2011.100.

I. Balaur, D. P. Nickerson, D. Welter, J. A. H. Wodke, F. Ancien, T. Gebhardt, V. Grouès, H. Hermjakob, M. König, N. Radde, A. Rougny, R. Schneider, R. S. Malik-Sheriff, K. B. Shiferaw, M. Stefan, V. Satagopam, and D. Waltemath. FAIRification of computational models in biology, Mar. 2025.

F. T. Bergmann, R. Adams, S. Moodie, J. Cooper, M. Glont, M. Golebiewski, M. Hucka, C. Laibe, A. K. Miller, D. P. Nickerson, B. G. Olivier, N. Rodriguez, H. M. Sauro, M. Scharm, S. Soiland-Reyes, D. Waltemath, F. Yvon, and N. Le Novère. COMBINE archive and OMEX format: One file to share all information to reproduce a modeling project. *BMC bioinformatics*, 15(1):369, Dec. 2014. ISSN 1471-2105. doi: 10.1186/s12859-014-0369-z.

F. T. Bergmann, N. Rodriguez, and N. Le Novère. COMBINE Archive Specification Version 1. *Journal of Integrative Bioinformatics*, 12(2):261, Sept. 2015. ISSN 1613-4516. doi: 10.2390/biecoll-jib-2015-261.

J. K. Doig, R. J. MacFadyen, C. S. Sweet, K. R. Lees, and J. L. Reid. Dose-ranging study of the angiotensin type I receptor antagonist losartan (DuP753/MK954), in salt-deplete normal man. *Journal of Cardiovascular Pharmacology*, 21(5):732–738, May 1993. ISSN 0160-2446. doi: 10.1097/00005344-199305000-00007.

M. Donzelli, A. Derungs, M.-G. Serratore, C. Noppen, L. Nezic, S. Krähenbühl, and M. Haschke. The basel cocktail for simultaneous phenotyping of human cytochrome P450 isoforms in plasma, saliva and dried blood spots. *Clinical pharmacokinetics*, 53(3):271–282, Mar. 2014. ISSN 1179-1926 0312-5963. doi: 10.1007/s40262-013-0115-0.

FDA. FDA1995S60 - 020386Orig1s000rev - COZAAR FDA Review. https://www.accessdata.fda.gov/drugsatfda_docs/nda/96/020386Orig1s000rev.pdf, Apr. 1995a.

FDA. FDA1995S67 - 020386Orig1s000rev - COZAAR FDA Review. https://www.accessdata.fda.gov/drugsatfda_docs/nda/96/020386Orig1s000rev.pdf, Apr. 1995b.

T. L. Fischer, J. A. Pieper, D. W. Graff, J. E. Rodgers, J. D. Fischer, K. J. Parnell, J. A. Goldstein, R. Greenwood, and J. H. Patterson. Evaluation of potential losartan-phenytoin drug interactions in healthy volunteers. *Clinical pharmacology and therapeutics*, 72(3):238–246, Sept. 2002. ISSN 0009-9236. doi: 10.1067/mcp.2002.127945.

M. T. Göktaş, F. Pepedil, Ö. Karaca, S. Kalkışım, L. Cevik, E. Gumus, G. S. Guven, M. O. Babaoglu, A. Bozkurt, and U. Yasar. Relationship between genetic polymorphisms of drug efflux transporter MDR1 (ABCB1) and response to losartan in hypertension patients. *European Review for Medical and Pharmacological Sciences*, 20(11):2460–2467, June 2016. ISSN 2284-0729.

M. R. Goldberg, T. E. Bradstreet, E. J. McWilliams, W. K. Tanaka, S. Lipert, T. D. Bjornsson, S. A. Waldman, B. Osborne, L. Pivadori, and G. Lewis. Biochemical effects of losartan, a nonpeptide angiotensin II receptor antagonist, on the renin-angiotensin-aldosterone system in hypertensive patients. *Hypertension (Dallas, Tex.: 1979)*, 25(1):37–46, Jan. 1995a. ISSN 0194-911X. doi: 10.1161/01.hyp.25.1.37.

M. R. Goldberg, M. W. Lo, T. E. Bradstreet, M. A. Ritter, and P. Höglund. Effects of cimetidine on pharmacokinetics and pharmacodynamics of losartan, an AT1-selective non-peptide angiotensin II receptor antagonist. *European journal of clinical pharmacology*, 49(1-2):115–119, 1995b. ISSN 0031-6970. doi: 10.1007/BF00192369.

J. Grzegorzewski, J. Brandhorst, K. Green, D. Eleftheriadou, Y. Duport, F. Barthorscht, A. Köller, D. Y. J. Ke, S. De Angelis, and M. König. PK-DB: Pharmacokinetics database for individualized and stratified computational modeling. *Nucleic Acids Research*, 49(D1):D1358–D1364, Jan. 2021. ISSN 1362-4962. doi: 10.1093/nar/gkaa990.

Y. Han, D. Guo, Y. Chen, Y. Chen, Z.-R. Tan, and H.-H. Zhou. Effect of silymarin on the pharmacokinetics of losartan and its active metabolite E-3174 in healthy Chinese volunteers. *European journal of clinical pharmacology*, 65(6):585–591, June 2009. ISSN 1432-1041 0031-6970. doi: 10.1007/s00228-009-0624-9.

V. Haufroid. Genetic polymorphisms of ATP-binding cassette transporters ABCB1 and ABCC2 and their impact on drug disposition. *Current Drug Targets*, 12(5):631–646, May 2011. ISSN 1873-5592. doi: 10.2174/138945011795378487.

H.-X. Huang, H. Wu, Y. Zhao, T. Zhou, X. Ai, Y. Dong, Y. Zhang, and Y. Lai. Effect of CYP2C9 genetic polymorphism and breviscapine on losartan pharmacokinetics in healthy subjects. *Xenobiotica; the fate of foreign compounds in biological systems*, 51(5):616–623, May 2021. ISSN 1366-5928 0049-8254. doi: 10.1080/00498254.2021.1880670.

M. Hucka, F. T. Bergmann, C. Chaouiya, A. Dräger, S. Hoops, S. M. Keating, M. König, N. L. Novère, C. J. Myers, B. G. Olivier, S. Sahle, J. C. Schaff, R. Sheriff, L. P. Smith, D. Waltemath, D. J. Wilkinson, and F. Zhang. The Systems Biology Markup Language (SBML): Language

Specification for Level 3 Version 2 Core Release 2. *Journal of Integrative Bioinformatics*, 16(2), June 2019. ISSN 1613-4516. doi: 10.1515/jib-2019-0021.

S. M. Keating, D. Waltemath, M. König, F. Zhang, A. Dräger, C. Chaouiya, F. T. Bergmann, A. Finney, C. S. Gillespie, T. Helikar, S. Hoops, R. S. Malik-Sheriff, S. L. Moodie, I. I. Moraru, C. J. Myers, A. Naldi, B. G. Olivier, S. Sahle, J. C. Schaff, L. P. Smith, M. J. Swat, D. Thieffry, L. Watanabe, D. J. Wilkinson, M. L. Blinov, K. Begley, J. R. Faeder, H. F. Gómez, T. M. Hamm, Y. Inagaki, W. Liebermeister, A. L. Lister, D. Lucio, E. Mjolsness, C. J. Proctor, K. Raman, N. Rodriguez, C. A. Shaffer, B. E. Shapiro, J. Stelling, N. Swainston, N. Tanimura, J. Wagner, M. Meier-Schellersheim, H. M. Sauro, B. Palsson, H. Bolouri, H. Kitano, A. Funahashi, H. Hermjakob, J. C. Doyle, M. Hucka, and SBML Level 3 Community members. SBML Level 3: An extensible format for the exchange and reuse of biological models. *Molecular Systems Biology*, 16(8):e9110, Aug. 2020. ISSN 1744-4292. doi: 10.15252/msb.20199110.

M.-G. Kim, Y. Kim, J.-Y. Jeon, and D.-S. Kim. Effect of fermented red ginseng on cytochrome P450 and P-glycoprotein activity in healthy subjects, as evaluated using the cocktail approach. *British journal of clinical pharmacology*, 82(6):1580–1590, Dec. 2016. ISSN 1365-2125 0306-5251. doi: 10.1111/bcp.13080.

M. Kobayashi, M. Takagi, K. Fukumoto, R. Kato, K. Tanaka, and K. Ueno. The effect of bucolome, a CYP2C9 inhibitor, on the pharmacokinetics of losartan. *Drug metabolism and pharmacokinetics*, 23(2):115–119, 2008. ISSN 1880-0920 1347-4367. doi: 10.2133/dmpk.23.115.

M. König. Sbmlsim: SBML simulation made easy. Zenodo, Sept. 2021.

M. König. Sbmlutils: Python utilities for SBML. Zenodo, Aug. 2024.

M. König, A. Dräger, and H.-G. Holzhütter. CySBML: A Cytoscape plugin for SBML. *Bioinformatics*, 28(18):2402–2403, Sept. 2012. ISSN 1367-4811, 1367-4803. doi: 10.1093/bioinformatics/bts432.

C. R. Lee, J. A. Pieper, A. L. Hinderliter, J. A. Blaisdell, and J. A. Goldstein. Losartan and E3174 pharmacokinetics in cytochrome P450 2C9*1/*1, *1/*2, and *1/*3 individuals. *Pharmacotherapy*, 23(6):720–725, June 2003. ISSN 0277-0008. doi: 10.1592/phco.23.6.720.32187.

Z. Li, G. Wang, L.-S. Wang, W. Zhang, Z.-R. Tan, L. Fan, B.-L. Chen, Q. Li, J. Liu, J.-H. Tu, D.-L. Hu, Z.-Q. Liu, and H.-H. Zhou. Effects of the CYP2C9*13 allele on the pharmacokinetics of losartan in healthy male subjects. *Xenobiotica; the fate of foreign compounds in biological systems*, 39(10): 788–793, Oct. 2009. ISSN 1366-5928 0049-8254. doi: 10.1080/00498250903134435.

M. W. Lo, M. R. Goldberg, J. B. McCrea, H. Lu, C. I. Furtek, and T. D. Bjornsson. Pharmacokinetics of losartan, an angiotensin II receptor antagonist, and its active metabolite EXP3174 in humans. *Clinical pharmacology and therapeutics*, 58(6):641–649, Dec. 1995. ISSN 0009-9236. doi: 10.1016/0009-9236(95)90020-9.

M. McIntyre, S. E. Caffe, R. A. Michalak, and J. L. Reid. Losartan, an orally active angiotensin (AT1) receptor antagonist: A review of its efficacy and safety in essential hypertension. *Pharmacology & therapeutics*, 74(2):181–194, 1997. ISSN 0163-7258. doi: 10.1016/s0163-7258(97)82002-5.

A. Munafo, Y. Christen, J. Nussberger, L. Y. Shum, R. M. Borland, R. J. Lee, B. Waeber, J. Biollaz, and H. R. Brunner. Drug concentration response relationships in normal volunteers after oral administration of losartan, an angiotensin II receptor antagonist. *Clinical pharmacology and therapeutics*, 51(5):513–521, May 1992. ISSN 0009-9236. doi: 10.1038/clpt.1992.56.

M. L. Neal, M. König, D. Nickerson, G. Mısırlı, R. Kalbasi, A. Dräger, K. Atalag, V. Chelliah, M. T. Cooling, D. L. Cook, S. Crook, M. de Alba, S. H. Friedman, A. Garny, J. H. Gennari, P. Gleeson, M. Golebiewski, M. Hucka, N. Juty, C. Myers, B. G. Olivier, H. M. Sauro, M. Scharm, J. L. Snoep, V. Touré, A. Wipat, O. Wolkenhauer, and D. Waltemath. Harmonizing semantic annotations for computational models in biology. *Briefings in Bioinformatics*, 20(2):540–550, Mar. 2019. ISSN 1477-4054. doi: 10.1093/bib/bby087.

M. L. Neal, J. H. Gennari, D. Waltemath, D. P. Nickerson, and M. König. Open modeling and exchange (OMEX) metadata specification version 1.0. *Journal of Integrative Bioinformatics*, 17 (2-3), June 2020. doi: 10.18452/32800.

K.-S. Oh, S.-J. Park, D. D. Shinde, J.-G. Shin, and D.-H. Kim. High-sensitivity liquid chromatography-tandem mass spectrometry for the simultaneous determination of five drugs and their cytochrome P450-specific probe metabolites in human plasma. *Journal of chromatography. B, Analytical technologies in the biomedical and life sciences*, 895–896:56–64, May 2012. ISSN 1873-376X 1570-0232. doi: 10.1016/j.jchromb.2012.03.014.

M. Ohtawa, F. Takayama, K. Saitoh, T. Yoshinaga, and M. Nakashima. Pharmacokinetics and biochemical efficacy after single and multiple oral administration of losartan, an orally active nonpeptide angiotensin II receptor antagonist, in humans. *British journal of clinical pharmacology*, 35(3):290–297, Mar. 1993. ISSN 0306-5251 1365-2125. doi: 10.1111/j.1365-2125.1993.tb05696.x.

A. A. Pedro, T. W. Gehr, D. F. Brophy, and D. A. Sica. The pharmacokinetics and pharmacodynamics of losartan in continuous ambulatory peritoneal dialysis. *Journal of clinical pharmacology*, 40(4): 389–395, Apr. 2000. ISSN 0091-2700. doi: 10.1177/00912700022009099.

E. Puris, M. Pasanen, V.-P. Ranta, M. Gynther, A. Petsalo, P. Käkelä, V. Männistö, and J. Pihlajamäki. Laparoscopic Roux-en-Y gastric bypass surgery influenced pharmacokinetics of several drugs given as a cocktail with the highest impact observed for CYP1A2, CYP2C8 and CYP2E1 substrates. *Basic & clinical pharmacology & toxicology*, 125(2):123–132, Aug. 2019. ISSN 1742-7843 1742-7835. doi: 10.1111/bcpt.13234.

K. Sekino, T. Kubota, Y. Okada, Y. Yamada, K. Yamamoto, R. Horiuchi, K. Kimura, and T. Iga. Effect of the single CYP2C9*3 allele on pharmacokinetics and pharmacodynamics of losartan in healthy Japanese subjects. *European journal of clinical pharmacology*, 59(8-9):589–592, Nov. 2003. ISSN 0031-6970. doi: 10.1007/s00228-003-0664-5.

H.-B. Shin, E. H. Jung, P. Kang, C. W. Lim, K.-Y. Oh, C.-K. Cho, Y. J. Lee, C.-I. Choi, C.-G. Jang, S.-Y. Lee, and J.-W. Bae. ABCB1 c.2677G>T/c.3435C>T diplotype increases the early-phase oral absorption of losartan. *Archives of pharmacal research*, 43(11):1187–1196, Nov. 2020. ISSN 1976-3786 0253-6269. doi: 10.1007/s12272-020-01294-3.

D. A. Sica, M. W. Lo, W. C. Shaw, W. F. Keane, T. W. Gehr, C. E. Halstenson, K. Lipschutz, C. I. Furtek, M. A. Ritter, and S. Shahinfar. The pharmacokinetics of losartan in renal insufficiency. *Journal of hypertension. Supplement : official journal of the International Society of Hypertension*, 13(1):S49–52, July 1995. ISSN 0952-1178. doi: 10.1097/00004872-199507001-00007.

D. A. Sica, T. W. B. Gehr, and S. Ghosh. Clinical pharmacokinetics of losartan. *Clinical pharmacokinetics*, 44(8):797–814, 2005. ISSN 0312-5963. doi: 10.2165/00003088-200544080-00003.

L. P. Smith, M. Hucka, S. Hoops, A. Finney, M. Ginkel, C. J. Myers, I. Moraru, and W. Liebermeister. SBML Level 3 package: Hierarchical Model Composition, Version 1 Release 3. *Journal of Integrative Bioinformatics*, 12(2):268, Sept. 2015. ISSN 1613-4516. doi: 10.2390/biecoll-jib-2015-268.

E. T. Somogyi, J.-M. Bouteiller, J. A. Glazier, M. König, J. K. Medley, M. H. Swat, and H. M. Sauro. libRoadRunner: A high performance SBML simulation and analysis library. *Bioinformatics*, 31(20): 3315–3321, Oct. 2015. ISSN 1367-4811, 1367-4803. doi: 10.1093/bioinformatics/btv363.

S. Tanaka, S. Uchida, N. Inui, K. Takeuchi, H. Watanabe, and N. Namiki. Simultaneous LC-MS/MS analysis of the plasma concentrations of a cocktail of 5 cytochrome P450 substrate drugs and their metabolites. *Biological & pharmaceutical bulletin*, 37(1):18–25, 2014. ISSN 1347-5215 0918-6158. doi: 10.1248/bpb.b13-00401.

C. Welsh, J. Xu, L. Smith, M. König, K. Choi, and H. M. Sauro. libRoadRunner 2.0: A high performance SBML simulation and analysis library. *Bioinformatics*, 39(1):btac770, Jan. 2023. ISSN 1367-4811. doi: 10.1093/bioinformatics/btac770.

U. Yasar, M.-L. Dahl, M. Christensen, and E. Eliasson. Intra-individual variability in urinary losartan oxidation ratio, an in vivo marker of CYP2C9 activity. *British journal of clinical pharmacology*, 54 (2):183–185, Aug. 2002a. ISSN 0306-5251 1365-2125. doi: 10.1046/j.1365-2125.2002.01646.x.

U. Yasar, C. Forslund-Bergengren, G. Tybring, P. Dorado, A. Llerena, F. Sjöqvist, E. Eliasson, and M.-L. Dahl. Pharmacokinetics of losartan and its metabolite E-3174 in relation to the CYP2C9 genotype. *Clinical pharmacology and therapeutics*, 71(1):89–98, Jan. 2002b. ISSN 0009-9236. doi: 10.1067/mcp.2002.121216.

T. Yoshitani, H. Yagi, N. Inotsume, and M. Yasuhara. Effect of experimental renal failure on the pharmacokinetics of losartan in rats. *Biological & pharmaceutical bulletin*, 25(8):1077–1083, Aug. 2002. ISSN 0918-6158. doi: 10.1248/bpb.25.1077.